Influence of surface optical phonon on the electronic surface states in wurtzite group-III nitride ternary mixed crystals*

LI Gen-xiao (李根小) **and YAN Zu-wei** (闫祖威)**
College of Science, Inner Mongolia Agricultural University, Hohhot 010018, China

(Received 15 October 2019; Revised 17 February 2020)

An intermediate-coupling variational method is presented to investigate the surface electron states in wurtzite $A_xB_{1-x}N$ (A, B=Al, Ga and In) ternary mixed crystals (TMCs). Corresponding effective Hamiltonian are derived by considering the surface-optical-phonon (SO-phonon) influence and anisotropic structural effect. The surface-state energies of electron, the coupling constants and the average penetrating depths of the electronic surface-state wave functions have been numerical computed as a function of the composition x and the surface potential V_0 for the wurtzite $Al_xGa_{1-x}N$, $Al_xIn_{1-x}N$ and $In_xGa_{1-x}N$, respectively. The results show that the surface-state levels of electron are reduced with the increasing of the composition x in wurtzite $A_xB_{1-x}N$. It is also found that the electron-surface-optical-phonon (e-SO-p) coupling lowers the surface-state energies of electron and the shifts of the electronic surface-state energy level in the wurtzite $Al_xGa_{1-x}N$ and $Al_xIn_{1-x}N$ increase with the increasing of the composition x. However, in the wurtzite $In_xGa_{1-x}N$, the case is contrary. The influence of the e-SO-p interaction on the surface electron states can not be neglected in wurtzite $A_xB_{1-x}N$.

Document code: A **Article ID:** 1673-1905(2021)01-0022-7
DOI https://doi.org/10.1007/s11801-021-9177-7

The wide band-gap III-V compounds of semiconductors have become vital materials for their application in the field of the optoelectronic devices in the spectral region of green, blue and ultraviolet[1,2]. TMCs can play important roles in the modern electronics. Their properties can be varied by changing their composition. Vast researches involve the lattice dynamics of TMCs materials have been conducted in experimentally and theoretically. The III-nitride (III-N) TMCs, such as $Al_xGa_{1-x}N$, $Al_xIn_{1-x}N$ and $In_xGa_{1-x}N$, have got particular interest in recent years. The polar III-N TMCs have a direct band gap over a wide range that minimum gap is 1.97 eV for InN, the maximum value is 6.20 eV for AlN and an intermediate value is 3.39 eV for GaN in whole range of composition. The III-N TMCs provide more flexible opportunities for continuous layers in heterostructures and quantum wells with desirable lattice constants and band offsets, which permits for potential application of the III-N compounds in light-emitting and laser diodes[3,4]. In the $A_xB_{1-x}N$ (A, B=Al, Ga and In) TMCs, phonon modes and electron-phonon (e-p) coupling have been studied theoretically within the framework of modified random-element-isodisplacement (MREI) model[5-7]. The nitride semiconductors appear two natural crystal structures which hexagonal and cubic structure and display many unusual properties in III-V compounds. Due to the lower symmetries of the wurtzite phase, it has more complicated phonon dynamics and carrier-phonon interactions comparing the zinc-blende one. The wurtzite nitride crystals have a significant anisotropic influence on the effective mass of polaron compared with the other III-V semiconductors. The phonon branches are more distinct in the wurtzite nitride semiconductors and their TMCs. Over the past decades, the wurtzite nitride semiconductors have appeared as a matter of broad experimental and theoretical interests about their polaronic property, electronic effective mass, interface-phonon and e-p scatter[8-10].

The intrinsic electronic surface-states in polar crystals have attracted particular investigation by experimental and theoretical scientists. Their energy levels, state densities and existence conditions have been published[11-13]. It is recognized that the termination of the lattice give rise to the intrinsic surface electron states whose wave functions are localized in the near of the surface and decay rapidly inside the materials. As we known that the e-p

* This work has been supported by the Research Program of Science and Technology at Universities of Inner Mongolia Autonomous Region (No.NJZY16071), the Natural Science Foundation of Inner Mongolia (No.2020MS01008), and the National Natural Science Foundation Project of China (No.11664030).
** E-mail: zwyan@imau.edu.cn

interaction influences the electronic characteristics obviously and produces polaronic states in polar crystals. Furthermore, the features of the e-p scatter in semi-infinite material are quite differ from those in bulk one duo to the presence of surface. Surface modes of phonon appears and play an important role in determining the polaronic properties around a surface. The nearly-free-electron approximation (NFEA) and the variational approach were used to treat the influences of the e-p interaction and hydrostatic pressure on intrinsic surface-states in III-N compound semiconductors[14,15]. The results show that the e-p interaction lowers the surface-state energy levels and the SO-phonon contribution on the surface-state of electron is dominant, in specially, for the semiconductors which has strong e-p coupling and wide band gap. Many scientists researched the characteristics of polaron in the GaN, AlN and InN. However, in wurtzite $A_xB_{1-x}N$ (A, B=Al, Ga and In), the influence of the e-p interaction on the electronic surface-state is not mentioned in the previous investigations[16,17]. For wurtzite $A_xB_{1-x}N$, in researching the features of the electronic surface-states, it is necessary to account the influence of the e-SO-p coupling and structural anisotropy.

In this article, we have investigate the influence of the e-p interaction on the surface electron state in wurtzite III-N TMCs by using a variational method within the framework of the dielectric continuum model[18]. The influence of structural anisotropy and e-SO-p interaction are considered. An effective Hamiltonian for this e-p system introduced by Lee-Low-Pines (LLP)-like treatment[19]. A variational calculation for the electronic surface-state energies, shifts of the electronic surface-state energy level, coupling constants and average penetrating depths of the electronic surface-state wave functions in wurtzite III-N TMCs was performed. The numerical computation results for the wurtzite $Al_xGa_{1-x}N$, $Al_xIn_{1-x}N$ and $In_xGa_{1-x}N$ are given as function of the composition x and discussed.

Assuming a semi-infinite semiconductor system, in which the positive-half space ($z\geq 0$) is occupying with TMCs $A_xB_{1-x}N$, while the negative-half region ($z\leq 0$) is the vacuum. The materials have the translational symmetry in the surface plane and the symmetry has been broken along the direction perpendicular to the surface. We take the anisotropic axis as the z axis and denote its perpendicular direction as $\perp$. An electron moves in the material and couples with lattice vibrations. Using the NFEA, such an e-p interaction Hamiltonian can be presented as[11]

$$H=H_{\rm e}+H_{\rm ph}+H_{\rm e\text{-}p}, \tag{1}$$

where $H_{\rm e}$ is the free electronic Hamiltonian and is given in the follow form

$$H_{\rm e}=\frac{p_{\perp}^2}{2m_{\perp}^*}+\frac{p_z^2}{2m_{0z}}+V(z), \tag{2}$$

where $p_{\perp}$ and p_z are the components of the electronic momentum in the x-y plane and z orientation, and $m_{\perp}^*$ is the electronic band mass in the two band model with rest mass m_{0z}, respectively. The one-dimensional pseudo-potential $V(z)$ describing the potential experienced by the electron in the z orientation can be written as[14]

$$V(z)=\begin{cases}-2V_1\cos(2\pi z/c), & z\geq 0\\ V_0, & z\leq 0\end{cases}, \tag{3}$$

where c is the lattice constant of the polar crystal in z orientation, $V_1=E_g/2$ (E_g refers to the forbidden band gap of material) and V_0 are the vacuum energy levels in the two band models, respectively. $H_{\rm ph}$ in Eq.(1) is the SO-phonon field Hamiltonian and can be expressed as

$$H_{\rm ph}=H_{\rm SO}=\sum_k \hbar\omega_{\rm SO}a_k^+a_k\,. \tag{4}$$

We only taking the SO-phonon effect into account for the e-p coupling. The last term in Eq.(1), the e-p interaction one, can be written as

$$H_{\rm e\text{-}ph}=H_{\rm e\text{-}SO}=\sum_k\left(F_s\frac{{\rm e}^{-D_s k|z|}}{k^{1/2}}{\rm e}^{{\rm i}\boldsymbol{k}\cdot\boldsymbol{\rho}}a_k+h.c.\right), \tag{5}$$

with

$$F_s=\left[\frac{4\pi e^2\hbar}{S\omega_{\rm SO}}C_s\right]^{1/2}, \tag{6}$$

$$C_s=\sqrt{\left(\omega_{\rm SO}^4-B_{\rm T}^2\omega_{\rm SO}^2+\omega_{\perp{\rm T}}^2\omega_{z{\rm T}}^2\right)^3\left(\omega_{\rm SO}^4-B_{\rm L}^2\omega_{\rm SO}^2+\omega_{\perp{\rm L}}^2\omega_{z{\rm L}}^2\right)}\Big/ \left\{\sqrt{\varepsilon_{\perp}^{\infty}\varepsilon_z^{\infty}}\left[\left(B_{\rm T}^2-B_{\rm L}^2\right)\omega_{\rm SO}^4+2\left(\omega_{\perp{\rm L}}^2\omega_{z{\rm L}}^2-\omega_{\perp{\rm T}}^2\omega_{z{\rm T}}^2\right)\omega_{\rm SO}^2+B_{\rm L}^2\omega_{\perp{\rm T}}^2\omega_{z{\rm T}}^2-B_{\rm T}^2\omega_{\perp{\rm L}}^2\omega_{z{\rm L}}^2\right]\right\}, \tag{7}$$

$$D_s=\begin{cases}\left[\dfrac{\varepsilon_{\perp}^{\infty}\left(\omega_{\rm SO}^2-\omega_{z{\rm T}}^2\right)\left(\omega_{\rm SO}^2-\omega_{\perp{\rm L}}^2\right)}{\varepsilon_z^{\infty}\left(\omega_{\rm SO}^2-\omega_{\perp{\rm T}}^2\right)\left(\omega_{\rm SO}^2-\omega_{z{\rm L}}^2\right)}\right]^{1/2}, & z\geq 0\\ 1, & z\leq 0\end{cases}, \tag{8}$$

$$\omega_{\rm SO}^2=\frac{\varepsilon_{\perp}^{\infty}\varepsilon_z^{\infty}B_{\rm L}^2-B_{\rm T}^2}{2\left(\varepsilon_{\perp}^{\infty}\varepsilon_z^{\infty}-1\right)}-\frac{\sqrt{\left[\varepsilon_{\perp}^{\infty}\varepsilon_z^{\infty}\left(\omega_{\perp{\rm L}}^2-\omega_{z{\rm L}}^2\right)-\left(\omega_{\perp{\rm T}}^2-\omega_{z{\rm T}}^2\right)\right]^2+4\varepsilon_{\perp}^{\infty}\varepsilon_z^{\infty}\left(\omega_{\perp{\rm L}}^2-\omega_{\perp{\rm T}}^2\right)\left(\omega_{z{\rm L}}^2-\omega_{z{\rm T}}^2\right)}}{2\left(\varepsilon_{\perp}^{\infty}\varepsilon_z^{\infty}-1\right)}, \tag{9}$$

$$B_j^2=\omega_{\perp j}^2+\omega_{zj}^2,\qquad j={\rm L,T}\,. \tag{10}$$

In Eqs.(4) and (5), a_k^+ and a_k represents the creation and annihilation operators of a SO-phonon with wave vector $\boldsymbol{k}$ and frequency $\omega_{\rm SO}$, S is the surface area of the lattice, and $\boldsymbol{r}=(\boldsymbol{\rho}, z)$, where $\boldsymbol{\rho}$ and z are the x-y plane and z components of the electron coordinates, respectively.

In order to simplify the computation for the influence of the e-SO-p scatter, we making two unitary transformations[14]. The first unitary transformation U_1 is to eliminate the $\boldsymbol{\rho}$ and given by

$$U_1=\exp\left(-{\rm i}\sum_k a_k^+a_k\boldsymbol{k}\cdot\boldsymbol{\rho}\right), \tag{11}$$

$$H_1=U_1^{-1}HU_1=\frac{\left(p_{\perp}-\sum_k\hbar\boldsymbol{k}a_k^+a_k\right)^2}{2m^*}+\frac{p_z^2}{2m_0}+V(Z)+\sum_k\hbar\omega_{\rm SO}a_k^+a_k+\sum_k\left(F_s\frac{{\rm e}^{-D_s k|z|}}{k^{1/2}}a_k+h.c.\right), \tag{12}$$

where $\boldsymbol{\rho}$ of the electron disappears.

We taking the second unitary transformation U_2 form is

$$U_2 = \exp\left(\sum_k a_k^+ f_k - a_k f_k^* \right). \tag{13}$$

Under the condition of the lower temperature limit for a slow-moving electron, we perform a variational treatment to solve the Hamiltonian H_1 on the trial state

$$\left|\psi\right\rangle = U_2 \left|0\right\rangle \left|\phi_\lambda(z)\right\rangle, \tag{14}$$

where $\left|0\right\rangle$ describes the zero-SO-phonon state and the $\left|\phi_\lambda(z)\right\rangle$ is the trial wave function in the z orientation for an electron, whose variational parameter is λ.

The corresponding total variational energy of the e-p coupling system has obtained by following routes

$$E_v = \left\langle \psi \left| H_1 \right| \psi \right\rangle = \left\langle \phi_\lambda(z) \left| H^* \right| \phi_\lambda(z) \right\rangle, \tag{15}$$

with

$$H^* = \left\langle 0 \left| U_2^{-1} H_1 U_2 \right| 0 \right\rangle = \frac{p_\perp^2}{2m_\perp^*} + \frac{p_z^2}{2m_{0z}} + V(z) + \sum_k \left(F_s \frac{\mathrm{e}^{-D_s k|z|}}{k^{1/2}} f_k + h.c. \right) + \frac{\hbar^2}{2m_\perp^*} \left(\sum_k f_k^2 k \right)^2 + \sum_k f_k^2 \left(\hbar\omega_{\mathrm{SO}} - \frac{\hbar \boldsymbol{k} \bullet \boldsymbol{p}_\perp}{m_\perp^*} + \frac{\hbar^2 k^2}{2m_\perp^*} \right), \tag{16}$$

where H^* represents a one-dimensional and two-band model Hamiltonian, including the e-p interaction and is named the effective polaron Hamiltonian. The displacement amplitude f_k and its conjugate f_k^* in Eq.(16) can be determined by using a variational treatment similar to that used by LLP method in the bulk-polaron problems[19] and requires

$$\frac{\partial H^*}{\partial f_k} = \frac{\partial H^*}{\partial f_k^*} = 0 \cdot \tag{17}$$

Without losing of generality in the following, we can put $p_\perp = 0$ since we concentrated only on the surface electronic state and the electron z-orientation motion and in the x-y plane is inconsequential. Hence, the effective Hamiltonian H^* of such an e-p system can be simplified to follows form

$$H^* = \frac{p_z^2}{2m_{0z}} + V(z) + V_{\mathrm{eff}}(z), \tag{18}$$

with

$$V_{\mathrm{eff}}(z) = -\alpha_s \hbar\omega_{\mathrm{SO}} \beta(z), \tag{19}$$

where $V_{\mathrm{eff}}(z)$ is an effective and z-orientation potential, α_s is the e-SO-p coupling constant and defined as[14]

$$\alpha_s = \frac{4e^2}{\hbar\omega_{\mathrm{so}}^2} \sqrt{\frac{m_\perp^*}{2\hbar\omega_{\mathrm{SO}}}} C_s, \tag{20}$$

where C_s and ω_{SO} have been defined in Eqs.(7) and (9), respectively.

The optical phonons exhibit one mode behavior in wurtzite $Al_xGa_{1-x}N$, $Al_xIn_{1-x}N$ and $In_xGa_{1-x}N$ according to the result in the MREI model[7]. In this case, we can assuming the influence of the value of the composition x is a linear independence on these parameters in the lattice constant, band gap, the electron effective mass, LO/TO-phonon frequency and the optical dielectric constant. The parameters of TMCs can be obtained from binary parameters using a linear interpolation

$$T_{\mathrm{A}_x\mathrm{B}_{1-x}\mathrm{N}} = xT_{\mathrm{AN}} + (1-x)T_{\mathrm{BN}}, \tag{21}$$

where $T_{\mathrm{A}_x\mathrm{B}_{1-x}\mathrm{N}}$ denotes the lattice constant, band gap, the electron effective mass, LO/TO-phonon frequency and the optical dielectric constant, T_{AN} and T_{BN} are the corresponding parameters in the binary crystals AN and BN, respectively.

Now let's start from H^* in Eq.(18) to compute the electronic surface-state energy level. The corresponding variational energy is given by

$$E_v = \left\langle \phi_\lambda(z) \left| H^* \right| \phi_\lambda(z) \right\rangle, \tag{22}$$

where the trial wave function $\left|\phi_\lambda(z)\right\rangle$ for the polaronic surface state can be chosen to be the following form[11]

$$\left|\phi_\lambda(z)\right\rangle = \begin{cases} A\mathrm{e}^{-\lambda_1 z} \cos(\pi z/c + \lambda_2), & z \geq 0 \\ B\mathrm{e}^{kz}, & z \leq 0 \end{cases}, \tag{23}$$

where A and B are the normalization constants of the wave function $\left|\phi_\lambda(z)\right\rangle$, and treat λ_1 and λ_2 as variational parameters to seek the surface electron state energy.

Inserting Eqs.(18) and (23) into Eq.(22), we can obtain the expectation value of H^*[14]

$$E_v = \frac{\hbar^2 A^2 \pi^2}{8m_{0z}c^2\lambda_1} - \frac{V_0 A^2 \cos^2\lambda_2}{2\left(\lambda_1 + \frac{\pi}{c}\tan\lambda_2\right)} - E_{\text{e-SO}} - \frac{V_1 A^2}{4} \times \left(\frac{\cos 2\lambda_2}{\lambda_1} + \frac{2\lambda_1}{\lambda_1^2 + \frac{\pi^2}{c^2}} + \frac{\lambda_1 \cos 2\lambda_2 - \frac{2\pi}{c}\sin 2\lambda_2}{\lambda_1^2 + \frac{4\pi^2}{c^2}} \right), \tag{24}$$

where $E_{\text{e-SO}} = \alpha_s \hbar\omega_{\mathrm{SO}} A^2 \left(I + g\cos^2\lambda_2\right)$ is the e-SO-p coupling contribution to the electronic surface state energy, I and g are defined alike to that in Ref.[14].

The average penetrating depth of the electronic surface-state wave function in the material is defined by

$$d = \left\langle \phi_\lambda(z) \left| z \right| \phi_\lambda(z) \right\rangle = \frac{A^2}{8\lambda_1^2} + \frac{A^2\left(\lambda_1^2 - \frac{\pi^2}{c^2}\right)_1 \cos 2\lambda_2 - \frac{2\pi A^2 \lambda_1}{c}\sin 2\lambda_2}{8\left(\lambda_1^2 + \frac{\pi^2}{c^2}\right)^2}. \tag{25}$$

In Eqs.(24) and (25), the variational parameters λ_i (i=1, 2) are determined by

$$\frac{\partial E_v}{\partial \lambda_i} = 0, \qquad i = 1, 2. \tag{26}$$

The complexity of Eq.(26) gives rise to necessity of numerical solutions to seek the minimum value of E_v, i.e., the electronic surface-state energy E_s.

Using a variational approach we have numerically computed the electronic surface-state energies, coupling

constants and the average penetrating depths of the electronic surface-state wave functions as function of the composition x and surface potential V_0 in the wurtzite TMCs, such as $Al_xGa_{1-x}N$, $Al_xIn_{1-x}N$ and $In_xGa_{1-x}N$, respectively. The parameters used in the calculations are listed in Tab.1—3[20,21] and the results are plotted in Figs.1—5. For the sake of understanding the effect of structural anisotropy, we have also calculated the same items in the zinc-blende structure.

Tab.1 The optical phonon energies of materials used in calculations measured in meV

Material	$\hbar\omega_{zL}$	$\hbar\omega_{zT}$	$\hbar\omega_{\perp T}$	$\hbar\omega_{\perp L}$
GaN	91.10	66.06	91.97	69.53
AlN	110.68	71.10	113.54	83.42
InN	72.63	54.91	73.75	57.88

Tab.2 The dielectric constants of materials used in calculations

Material	ε_z^0	$\varepsilon_\perp^0$	$\varepsilon_z^\infty=\varepsilon_\perp^\infty$
GaN	10.18	9.36	5.35
AlN	11.72	8.97	4.84
InN	14.70	13.64	8.40

Tab.3 The lattice constants, band gaps and effective masses of electrons of materials, where m^* is in the electron rest mass m_0

Material	c (nm)	E_g (meV)	$m_\perp^*=m_{0z}^*$
GaN	0.518	3390	0.20
AlN	0.4982	6200	0.30
InN	0.5760	1970	0.12

To clearly understand the influence of the e-SO-p coupling on the surface-states of electron, in Fig.1, we have plotted the electronic surface-state energy levels E_s with and without the SO-phonon influence as a function of the composition x with V_0=5.0 eV for the wurtzite and zinc-blende $Al_xGa_{1-x}N$, $Al_xIn_{1-x}N$ and $In_xGa_{1-x}N$, respectively[11]. Fig.1 shows that E_s are almost linear decreases with the increasing of the composition x for $Al_xGa_{1-x}N$ and $In_xGa_{1-x}N$, and are non-monotonous for $Al_xIn_{1-x}N$. The surface-state energy levels E_s with e-SO-p interaction are in the range of 1.342 eV to 0.644 eV, 1.327 eV to 0.645 eV and 1.342 eV to 1.328 eV for wurtzite $Al_xGa_{1-x}N$, $Al_xIn_{1-x}N$ and $In_xGa_{1-x}N$ while the composition x increases from 0 to 1 and the net decrease is 52.0%, 51.4% and 1.0%, respectively. The values of the E_s without e-p coupling varies from 1.386 eV to 0.732 eV, from 1.338 eV to 0.733 eV and from 1.386 eV to 1.339 eV for wurtzite $Al_xGa_{1-x}N$, $Al_xIn_{1-x}N$ and $In_xGa_{1-x}N$, respectively. It also gives that E_s for wurtzite $Al_xGa_{1-x}N$, $Al_xIn_{1-x}N$ and $In_xGa_{1-x}N$ are less than that for zinc-blende cases. The electronic surface-state energy levels E_s with the SO-phonon contribution in wurtzite materials are lower than that for corresponding zinc-blende one for 475 meV, 381 meV and 387 meV for $Al_xGa_{1-x}N$, $Al_xIn_{1-x}N$ and $In_xGa_{1-x}N$ at x=0.20. It is follows that the broader the forbidden band gap or the stronger the e-p interaction, the lower are the electronic surface-state energy levels.

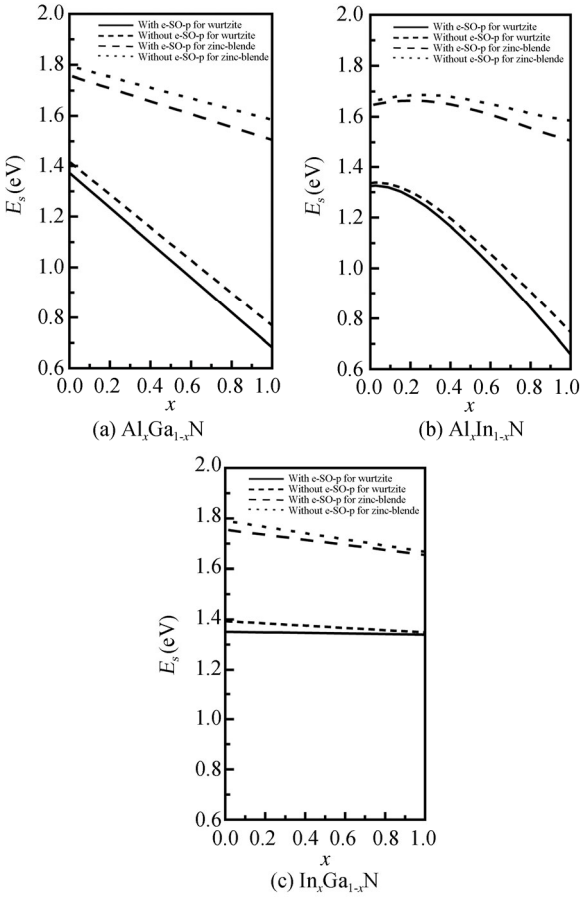

Fig.1 The electronic surface state energy levels E_s with and without e-SO-p interactions for wurtzite structures, and with and without e-SO-p interactions for zinc-blende structures as functions of the composition x for several III-N TMCs

In Fig.2, we have illustrated the shifts of the electronic surface-state energy level $E_{e\text{-}SO}$ as function of the composition x caused by the e-SO-p interaction with V_0=5.0 eV. Fig.2 shows that the e-SO-p interaction reduced the electronic surface-state energy levels for all computed $A_xB_{1-x}N$. In the other word, the electronic surface-state energy levels with the e-SO-p interaction are always less than that without SO-phonon effect. The two curves of the E_s with and without the influence of the e-SO-p interaction are divided distinctly from each other. The shifts of the electronic surface-state energy levels $E_{e\text{-}SO}$ are decades of meV for all aforementioned materials. $E_{e\text{-}SO}$ is 52.129 meV, 19.071 meV and 35.493 meV for wurtzite $Al_{0.20}Ga_{0.80}N$, $Al_{0.20}In_{0.80}N$ and $In_{0.20}Ga_{0.80}N$, respectively. The shift of the electronic surface-state energy levels $E_{e\text{-}SO}$ is related to SO-phonon energy $\hbar\omega_{SO}$ and e-SO-p coupling constant α_S. The SO-phonon energy and e-SO-p coupling constant are increased with the in-

creasing of the composition, for the wurtzite$Al_xGa_{1-x}N$ and $Al_xIn_{1-x}N$, respectively. It caused the increasing of $E_{e\text{-}SO}$ with the composition x, as Fig.2(a) and (b) shown, for the wurtzite$Al_xGa_{1-x}N$ and $Al_xIn_{1-x}N$, respectively. At x=0.0, the shifts of the electronic surface-state energy levels are $E_{e\text{-}SO}$=44.456 meV and 11.224 meV, and at x=1.0, they increase to 87.927 meV and 88.359 meV for wurtzite $Al_xGa_{1-x}N$ and $Al_xIn_{1-x}N$, respectively. For the wurtzite $In_xGa_{1-x}N$, the case is contrary, that $E_{e\text{-}SO}$ is decrease with the increasing of the composition x as the Fig.2(c) shows. It is due to the decrease of the SO-phonon energy and e-SO-p coupling constant with the increasing of the composition. The shifts are $E_{e\text{-}SO}$=44.456 meV and 11.075 meV at x=0.0 and 1.0, respectively. It indicates that the stronger e-p coupling is, the greater the shift of the electronic surface state energy level.

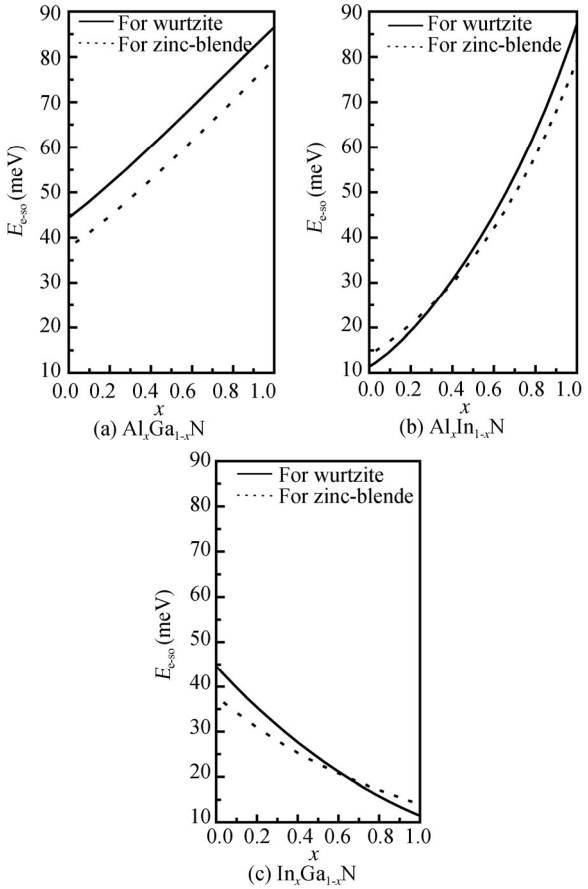

Fig.2 The shifts of the electronic surface state energy levels $E_{e\text{-}SO}$ for wurtzite and zinc-blende structures as functions of the composition x for several III-N TMCs

We have also numerical computed the electronic surface-state energy levels E_s as function of V_0. We have chosen the value of V_0 to vary in a reasonable range 3.9—5.6 eV[11]. The electronic surface-state energy levels and its shifts are shown in Figs.3 and 4 as function of the surface potential V_0 in the numerical computations, respectively. Fig.3 shows that the electronic surface-state energy levels E_s are linear increase with the increasing of V_0 at the composition x=0.55 for all calculated TMCs. It is also found, in Fig.3(a) and (b), that two curves of the surface-state energy level are separated distinctly from each other for $Al_{0.55}Ga_{0.45}N$ and $Al_{0.55}In_{0.45}N$. However, the corresponding curves in Fig.3(c) very close to each other for the $In_{0.55}Ga_{0.45}N$. It is clear that the e-p interaction lowers the electronic surface-state energy levels. The shifts of the electronic surface-state energy level $E_{e\text{-}SO}$ caused by the e-SO-phonon interaction in the surface of material are determined mainly by the SO-phonon energy and e-SO-phonon coupling constant. Hence, $E_{e\text{-}SO}$ are almost independent of surface potential V_0 as Fig.4 shows. The shift of the surface state energy level $E_{e\text{-}SO}$ is 67.637 meV, 41.428 meV and 22.445 meV for wurtzite $Al_{0.55}Ga_{0.45}N$, $Al_{0.55}In_{0.45}N$ and $In_{0.55}Ga_{0.45}N$ at V_0=5.0 eV, respectively.

Fig.5 gives the e-SO-p coupling constants α_s as function of the composition x, where V_0=5.0 eV. It is seen that there are monotonous changes of the e-SO-p coupling constant α_s with the composition x for all calculated materials. The e-SO-p coupling constant α_s is increase with the increasing of the composition x for $Al_xGa_{1-x}N$ and $Al_xIn_{1-x}N$. Nevertheless, for $In_xGa_{1-x}N$, α_s is become weak with the increasing of the composition x. It is also found that the e-SO-p coupling constants α_s in wurtzite materials is larger than that in zinc-blende structures in the whole range of the composition x. α_s equals to 0.758, 0.851, 0.497, 0.743, 0.818 and 0.441 for the wurtzite $Al_xGa_{1-x}N$, wurtzite $Al_xIn_{1-x}N$, wurtzite $In_xGa_{1-x}N$, zinc-blende $Al_xGa_{1-x}N$, zinc-blende $Al_xIn_{1-x}N$ and zinc-blende $In_xGa_{1-x}N$ at x=0.55 and with V_0=5.0 eV, respectively. The value of the e-SO-p coupling constant α_s gets the corresponding numerical value that in the end material AN and BN at x=0.0 and x=1.0.

We also computed the average penetrating depths of the electronic surface-state wave function d as function of the composition x. The result shows that the values of d are within the scope of 0.094—0.070 nm for wurtzite $Al_xGa_{1-x}N$, 0.134—0.069 nm for wurtzite $Al_xIn_{1-x}N$ and 0.094—0.138nm for wurtzite $In_xGa_{1-x}N$ in the entire range of composition x, respectively. Tab.4 shows the average penetrating depths d for aforesaid materials at x=0.55 and V_0=5.0 eV. The average penetrating depth is less than the lattice constant of material. It reveals that the wave function of the electronic surface-state is localizes near the surface.

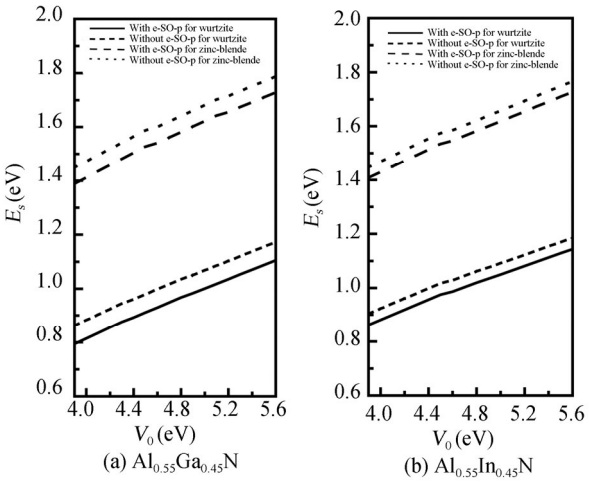

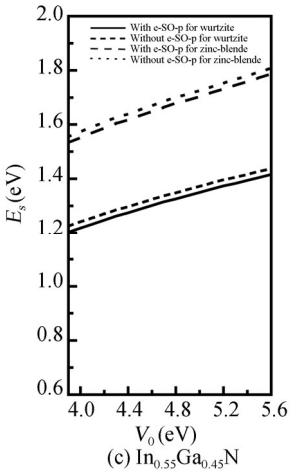

Fig.3 The electronic surface state energy levels E_s with and without e-SO-p interactions for wurtzite structures, and with and without e-SO-p interactions for zinc-blende structures as functions of the surface potential V_0 for several III-N TMCs

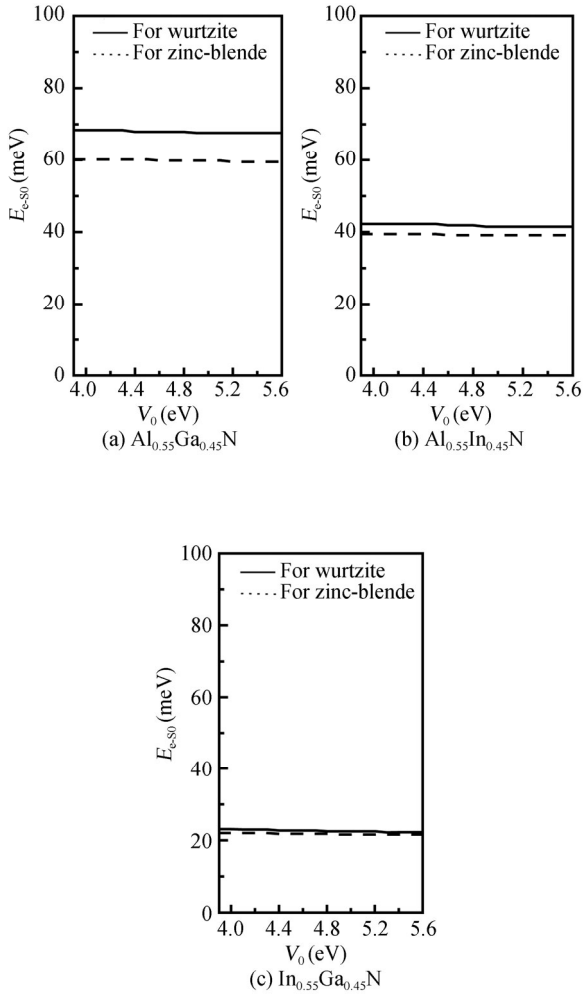

Fig.4 The shifts of the electronic surface state energy levels $E_{e\text{-}SO}$ for wurtzite and zinc-blende structures as functions of the surface potential V_0 for several III-N TMCs

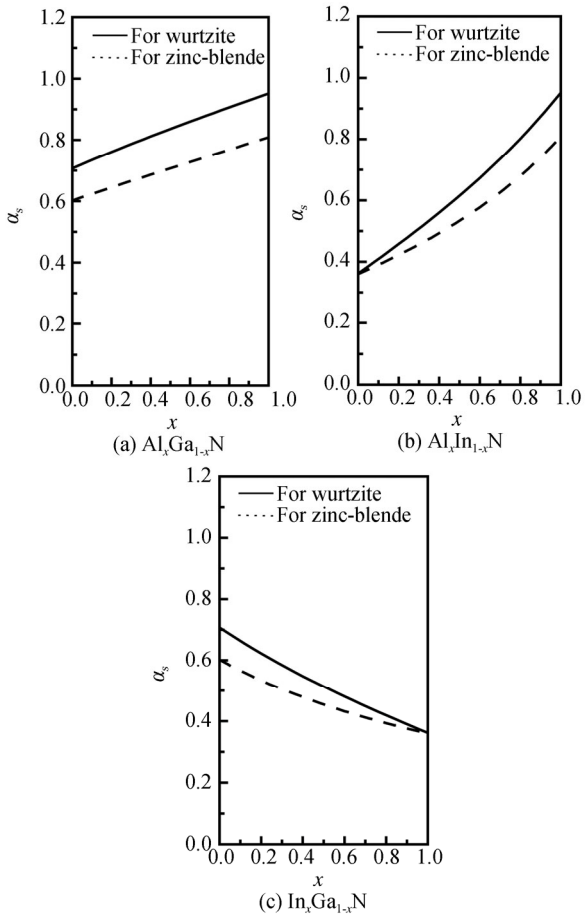

Fig.5 The e-SO-p coupling constants α_s for wurtzite and zinc-blende structures as functions of the composition x for several III-N TMCs

Tab.4 The average penetrating depth of the electronic surface state wave function d and lattice constant c for wurtzite $Al_xGa_{1-x}N$, $Al_xIn_{1-x}N$ and $In_xGa_{1-x}N$

Material	$Al_{0.55}Ga_{0.45}N$	$Al_{0.55}In_{0.45}N$	$In_{0.55}Ga_{0.45}N$
d (nm)	0.080	0.090	0.108
c (nm)	0.507	0.533	0.550

In summary, a variational treatment is presented to calculate the electronic surface-state energy level in wurtzite group-III nitride TMCs. The influence of the SO phonon on the electronic surface-state are obtained and discussed for $Al_xGa_{1-x}N$, $Al_xIn_{1-x}N$ and $In_xGa_{1-x}N$, respectively. The numerical results show that the electronic surface-state energy decrease with the increasing of the composition x in wurtzite III-N TMCs. It is also found that the electronic surface-state energy levels in wurtzite structural material are less than that in the zinc-blende counterparts. It is indicated that the e-SO-p interaction lowers the electronic surface-state energy levels. Hence the influence of the e-SO-p interaction and structural anisotropy on the electronic surface-state in wurtzite

III-N TMCs can not be neglected, especially for the semiconductors which have wide band gap and strong e-p coupling.

References

[1] Z. Li, H. H. Tan, C. Jagadish and L. Fu, Adv. Mater. Technol. **3**, 1 (2018).

[2] J.H. Liu, H. Zhang, X.L. Cheng and Y. Miyamoto, Phys. Rev. B **94**, 5404 (2016).

[3] S. Zhang, Y. Zhang, X. Chen, Y.N. Guo, J.C. Yan, J.X. Wang and J.M.Li, J. Semi. **11**,113002 (2017).

[4] J. Li, Y. Lv, C.F. Li, Z.W. Ji, Z.Y. Pang, X.G. Xu and M.S. Xu, Chinese Phys. B **9**, 098504 (2017).

[5] Z. Gu, S. L. Ban and D. D. Jiang, J. Appl. Phys. **121**, 035703 (2017).

[6] R. Singh, M. Dutta, M.A. Stroscio, A.G. Birdwell and P.M. Amirtharaj, J. Appl. Phys. **125**, 205704 (2019).

[7] H. Grille, C. Schnittler and F. Bechstedt, Phys. Rev. B **61**, 6091 (2000).

[8] J.J. Shi, Phys. Rev. B **68**, 165335 (2003).

[9] N. Armakavicius, V. Stanishev, S. Knight, P. Kuhne, M. Schubert and V. Darakchieva, Appl. Phys. Lett. **112**, 082103 (2018).

[10] Y.L. Li, P. Jin, G.P. Liu, W.Y. Wang, Z.Q. Qi, C.Q. Chen and Z.G. Wang, Chinese Phys. B **8**, 397 (2016).

[11] S.G. Davison and M. Steslicka, Basic Theory of Surface States, Clarendon Press, Oxford, 1992.

[12] A.B. Petrin, J. Exp. Theor. Phys. **116**, 486 (2013).

[13] R. Khordad and H. Bahramiyan, J. Appl. Phys. **115**, 124314 (2014).

[14] G.X. Li and Z.W. Yan, Superlattices Microst. **52**, 514 (2012).

[15] L. Zhang and J. J. Shi, J. Appl. Phys. **113**, 093710 (2013).

[16] Y. P. Fan and J.H. Hou, Mod. Phys. Lett. B **29**, 1550130 (2015).

[17] M. E. Mora-Ramos, V. R. Velasco and J. Tutor, Surf. Sci. **592**, 112 (2006).

[18] M. Born and K. Huang, Dynamical Theory of Crystal Lattices, Clarendon Press, Oxford, 1954.

[19] T.D. Lee, F.E. Low and D. Pines, Phys. Rev. **90**, 297 (1953).

[20] S. Strite and H. Morkoc, J. Vac. Sci. Technol. B **10**, 1237 (1992).

[21] I. Vurgaftman, J. R. Meyer and L. R. Ram-Mohan, J. Appl. Phys. **89**, 5815 (2001).